Oscillatory Decay of Magnetization Induced by Domain-Wall Stray Fields

Luc Thomas,[1] Jan Lüning,[1] Andreas Scholl,[2] Frithjof Nolting,[2] Simone Anders,[2] Joachim Stöhr,[1] and Stuart S. P. Parkin[1]

[1]*IBM Research Division, Almaden Research Center, San Jose, California 95120-6099*

[2]*Advanced Light Source, Lawrence Berkeley National Laboratory, Berkeley, California 94720*

(Received 20 October 1999)

The demagnetization of a hard ferromagnetic layer via the fringing fields of domain walls created by reversing the moment of a neighboring soft ferromagnetic layer is explored experimentally. An unusual oscillatory decay of the magnetic moment of the hard layer is observed using structures in which the demagnetization occurs after a few hundred cycles. This surprising observation is confirmed on a microscopic scale by detailed imaging of the magnetization of the hard layer using high resolution photoemission electron microscopy and by micromagnetic simulations.

PACS numbers: 75.70.–i, 75.60.Ch, 85.70.Kh

Indirect magnetic coupling in thin film magnetic multilayered structures is of considerable interest particularly because of its importance to magnetoresistive devices. In the past few years, much attention has been paid to oscillatory interlayer exchange coupling through nonmagnetic metallic spacer layers. This phenomenon has been studied extensively, both experimentally [1] and theoretically ([2] and references therein). However, simple magnetostatic interactions can also lead to strong coupling between ferromagnetic layers. These are of particular relevance to magnetic tunnel junctions (MTJ) in which two ferromagnetic (FM) layers are separated by a thin insulating layer [3]. For patterned structures with submicron lateral dimensions, stray magnetic fields from the edges can give rise to significant coupling between the FM layers [4]. Roughness of the FM/spacer interfaces may also result in interlayer coupling [5]. Finally, magnetic domain walls or vortices located in one of the FM layers may generate large stray fields in the neighboring FM layer and so induce another type of dipolar coupling [6,7].

The simplest type of MTJ is one comprised of "hard" and "soft" FM layers, which display significantly different switching fields. It was recently observed that the behavior of hard/soft MTJs was strongly affected by the repeated switching or cycling of the soft layer's magnetization [6]. This cycling was found to progressively demagnetize the hard magnetic layer, even though the cycling field was much too small to have any direct effect on the hard layer [8]. This phenomenon was not observed if the magnetization was reversed in a rotating field, suggesting an important role of domain walls nucleated in the soft layer during its switching. The influence of domain walls was established later using analytical calculations [7] and micromagnetic simulations [9]. Stray fields from domain walls in the soft layer were found to reach values as high as a few thousand Oersted locally within the hard layer, far exceeding the latter's coercive field. It was also found that the demagnetization rate of the hard layer was highly sensitive to the thickness of the FM layers, in excellent agreement with calculations of the domain wall stray field strengths and spatial extent [7].

In this Letter, we present a detailed analysis of the demagnetization process of hard $Co_{75}Pt_{12}Cr_{13}$ FM layers. Interestingly, we find that this magnetization decay exhibits an oscillatory behavior as the moment of a neighboring CoFe soft layer is successively cycled back and forth. Microscopic imaging of the hard layer using x-ray magnetic circular dichroism (XMCD) photoemission electron microscopy (PEEM) [10] confirms this macroscopic observation. These experimental results are in excellent agreement with micromagnetic calculations, which suggest that the demagnetization is related to the motion of vortices within the CoFe layer during its magnetization reversal.

Magnetic trilayers of 100 Å $Co_{84}Fe_{16}$/15 Å Cr/50 Å $Co_{75}Pt_{12}Cr_{13}$ were grown by dc magnetron sputtering in 10^{-3} Torr Ar on Si/SiO_2 wafers [6], and the sample was capped with 15 Å of Al to prevent oxidation. Note that the Cr spacer layer was thick enough to avoid either indirect electronic coupling or direct coupling through pinholes [11]. Moreover, related samples with insulating Al_2O_3 spacer layers exhibited similar properties. The hard FM layer was grown on top of the structure to make it accessible for PEEM, which detects secondary electrons produced during absorption of x rays, and so is surface sensitive [12]. The microscopy studies were carried out with the PEEM-II microscope at the Advanced Light Source in Berkeley, using 80% circularly polarized soft x rays from a bending magnet source [13]. XMCD-PEEM images were recorded at the Co $L_{2,3}$ absorption edges with the projection of the photon spin aligned along a particular direction, that of the initial macroscopic magnetization of the sample, and the direction of the applied field. The contrast was enhanced by dividing images obtained at the L_3 and L_2 edges [10]. Note that the Co signal is purely due to the hard FM layer as the $1/e$ sampling depth at these photon energies is only about 20 Å [12]. Moreover, no signal (from the soft CoFe layer) was observed at the Fe L edges.

The hysteresis loop shown in the inset in Fig. 1 is typical for a hard/soft magnetic sandwich. The FM layers switch independently at $H_c \sim 700$ Oe for the hard CoPtCr layer and $H_c \sim 50$ Oe for the soft CoFe layer. Thus, by cycling the applied field from $+200$ to -200 to $+200$ Oe

 0031-9007/00/84(15)/3462(4)$15.00

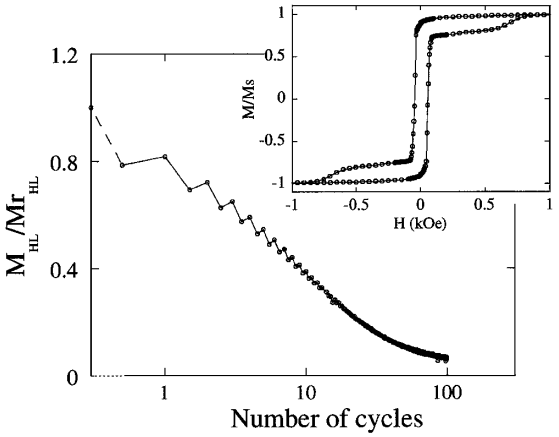

FIG. 1. Decay of the hard CoPtCr layer remanent magnetization M_{HL} upon cycling the soft CoFe layer's magnetization (± 200 Oe). The curve is normalized to Mr_{HL}, remanent magnetization before cycling. The number of cycles (plotted on a logarithmic scale for clarity) is indexed every $\frac{1}{2}$ cycle, which corresponds to each reversal of the CoFe layer. The inset shows the hysteresis loop of the structure, normalized to its saturation magnetization Ms.

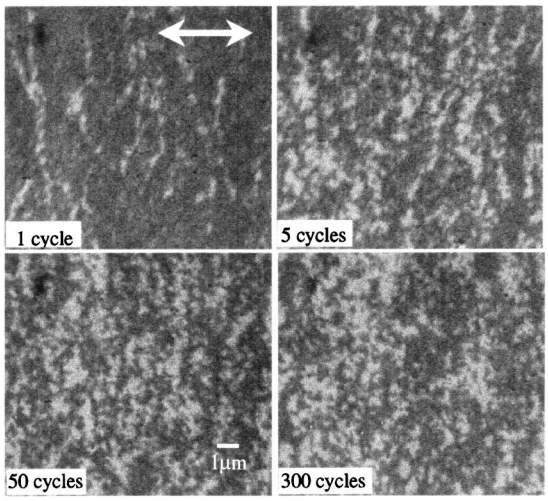

FIG. 2. PEEM images of a 10×11 μm^2 area of a CoPtCr layer of a CoPtCr/Cr/CoFe sandwich recorded at the indicated numbers of cycles of the field used to reverse the moment of the soft CoFe layer. The white arrow indicates the cycling field direction. Black and white areas correspond to the two orientations of the magnetization component parallel to the cycling field direction.

the magnetization of the soft CoFe layer can be cycled back and forth without directly switching the magnetic state of the hard layer. Nevertheless, remarkably, as shown in Fig. 1, the remanent magnetization of the hard layer decreases progressively with increasing numbers of cycles N_c of the soft layer moment. Note N_c is indexed every half integer, which corresponds to successive reversals of the CoFe layer magnetization. The decay of the magnetization is similar to that found previously for related hard/soft structures [6,7]. However, here we find an oscillating component to the evolution of the magnetization of the hard layer superimposed on its gradual decay. Switching the CoFe moment from + to − induces a large decay of the CoPtCr moment, while the reversal from − to + induces a smaller change, and for small N_c, even a partial remagnetization of the hard layer. This oscillating component is most apparent for small N_c when the demagnetization rate is sufficiently large, which occurs for samples with thin enough hard layers and spacer layers [7]. As can be seen from Fig. 1 the hard layer moment is reduced by half for $N_c \sim 10$ whereas in previous studies [6,7] the decay rate was much slower which is why the oscillatory component was not previously observed.

To understand the demagnetization process in more detail, PEEM images were recorded for various N_c. The sample was first prepared in a fully magnetized remanent state in a field of 5 kOe which here corresponds to a uniformly black PEEM image in which no significant structure was found. The cycling field of ± 200 Oe was then applied *in situ* so that changes in the magnetic state of the same area of the hard layer after each reversal of the soft layer magnetization could be imaged. The four images in Fig. 2 show a 10×11 μm^2 area of the film for $N_c = 1$, 5, 50, and 300. As N_c increases, regions with reversed magnetization (white areas) progressively expand. After about 50 cycles, the proportion of black and white regions is approximately the same, in good agreement with the small remanent magnetization measured for the same N_c (see Fig. 1). However, even though the net magnetization is close to zero, the magnetic state of the film continues to evolve with further field cycling. As shown in Fig. 2, the image recorded for 300 cycles is quite different from that for 50 cycles, even though the proportion of black and white regions is about the same. A particularly interesting feature of these images is the increase of disorder of the magnetization distribution with increasing N_c. For small N_c, regions with reversed magnetization appear to form strands approximately perpendicular to the net magnetization. This ordered structure is still weakly present for 50 cycles but has vanished completely for 300 cycles.

PEEM images of a representative 5×5 μm^2 area of the CoPtCr FM layer are shown in Fig. 3 recorded after every $\frac{1}{2}$ cycle for the first 3 cycles. After the first $\frac{1}{2}$ cycle (CoFe moment switched from + to −), reversed domains (white areas) appear very clearly, forming strands roughly perpendicular to the initial magnetization direction. When the CoFe magnetization is switched back to its original direction (1 cycle), only small changes are observed in the PEEM image. Indeed, the relative proportion of reversed domains tends to decrease as some of these domains have switched back to their initial orientation (see, for example, the highlighted part of the images). The next few cycles result in a similar behavior: switching the CoFe magnetization from + to − induces a large increase of reversed domains, while the reversal from − to + has a weaker impact, with a slight decrease of the overall area of reversed domains. Note that the shape of the reversed domains also changes. The strands of reversed moment tend to break into smaller domains alternating in direction. The

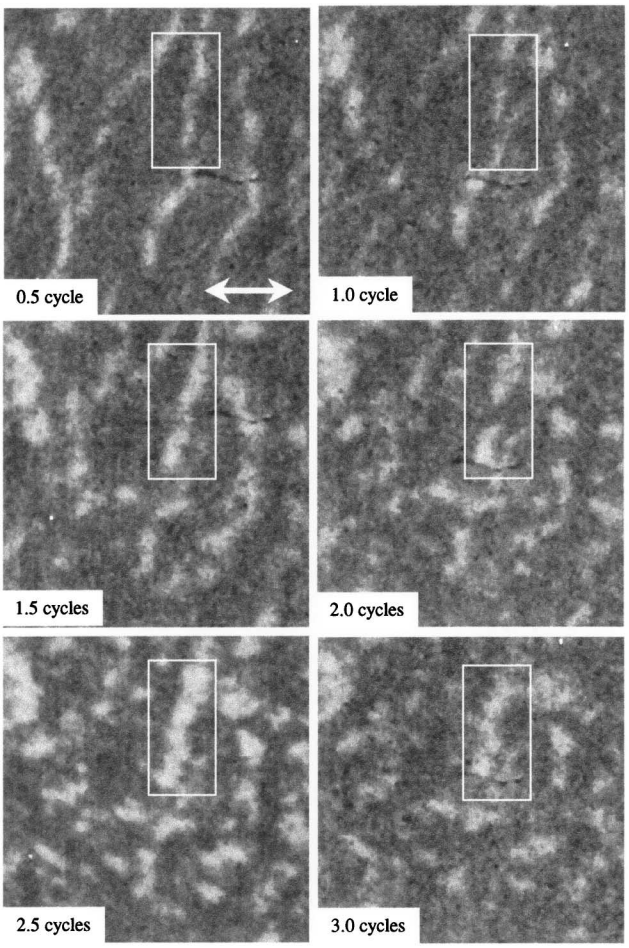

FIG. 3. PEEM images of the same 5×5 μm^2 area recorded at the indicated numbers of cycles. The white arrow indicates the cycling field direction. The white rectangle highlights the gradual evolution of one area of the magnetization of the hard layer as the soft CoFe layer moment is cycled back and forth.

oscillatory component of the magnetization decay, which is clearly observed on a microscopic scale in the PEEM images, is in excellent accord with the macroscopic magnetization measurements shown in Fig. 1.

CoPtCr films are known to have a granular structure [14]. The hard magnetic CoPt grains are surrounded by Cr-rich boundaries, which are weakly magnetic and strongly reduce exchange interactions between the CoPt grains. In the simplest model, the CoPt grains are coupled only by dipolar interactions. Note that the grain size of about 10–20 nm is not resolved by PEEM, whose resolution of about 50 nm limits us to resolve clusters of more tightly coupled grains. While dipolar interactions play an important role in the magnetization process of CoPtCr films, it is difficult to see how they could be responsible for the appearance of the strands of reversed magnetization shown in Figs. 2 and 3. Dipolar interactions would tend to favor the creation of reversed moment in the direction parallel rather than perpendicular to the net magnetization of the hard layer. However, perpendicular to the magnetization direction, dipolar interactions would tend to favor the antiparallel orientation of neighboring regions. Thus, it is possible to rationalize some of the features observed in the PEEM images in Fig. 3. In particular, the breaking up of strands perpendicular to the magnetization into smaller regions with alternating magnetic orientations and the broadening of the reversed domains along the magnetization direction (see, for example, the highlighted part of the images recorded at 0.5, 1.5, and 2.5 cycles) may be explained on the basis of dipolar interactions. These effects can be expected as the magnetization reversal is assisted by the dipolar fields of the neighboring reversed domains.

Neither the oscillatory behavior of the magnetization decay nor the apparition of the strands of reversed domains fit a simple model of domain-wall stray field induced coupling. In particular, if only Néel domain walls with single segments are considered, the in-plane stray fields from such walls will be perpendicular, and their sign will depend only on the chirality of the wall [7]. Thus, assuming an equal distribution of Néel walls of opposite chirality in the soft layer during its magnetization reversal, the decay of the hard layer's magnetization, within this model, would not depend on the switching direction of the soft layer and would thus exhibit a simple monotonic behavior. To clarify both this apparent discrepancy and the observation of the strands of reversed domains within the hard layer, micromagnetic simulations were performed on a model system. A magnetic trilayer of 100 Å CoPtCr/14 Å Cr/150 Å Co was considered with lateral dimensions $L_x = 640$ nm and $L_y = 1280$ nm. The CoPtCr layer is approximated by exchange-decoupled 10-nm-sized cubic grains with a three-dimensional random distribution of anisotropy axes. The same lateral cell size is used for the soft Co layer, within which the cells are exchange coupled while anisotropy is neglected. Periodic boundary conditions are applied along the magnetization direction x. A domain wall (DW) parallel to x is artificially generated by pinning the soft layer's magnetization in opposite directions, $M_x = 1$ at $y = 0$ and $M_x = -1$ at $y = L_y$. The external field is applied along x [see Fig. 4(c)], inducing DW motion along y. The hysteresis curve of such a system, calculated by solving the Landau-Lifschitz-Gilbert equation, is shown in Fig. 4(a) (details of the micromagnetic code can be found in Ref. [15]). Note that the experimental features of the hard/soft magnetic sandwich are well reproduced. First, the two layers have very different switching fields 1.2 and 0.2 kOe, respectively. Second, cycling the Co layer magnetization in ± 500 Oe induces an oscillatory demagnetization of the hard CoPtCr, in excellent agreement with the experimental results [Fig. 4(b)]. The domain structure of the CoPtCr shown in Fig. 4(d) for the first few cycles also agrees very well with the PEEM observations. The first switching of the Co layer induces the nucleation of linear-shaped domains with reversed magnetization (0.5 cycle), with these strands oriented perpendicular to the average magnetization direction. The

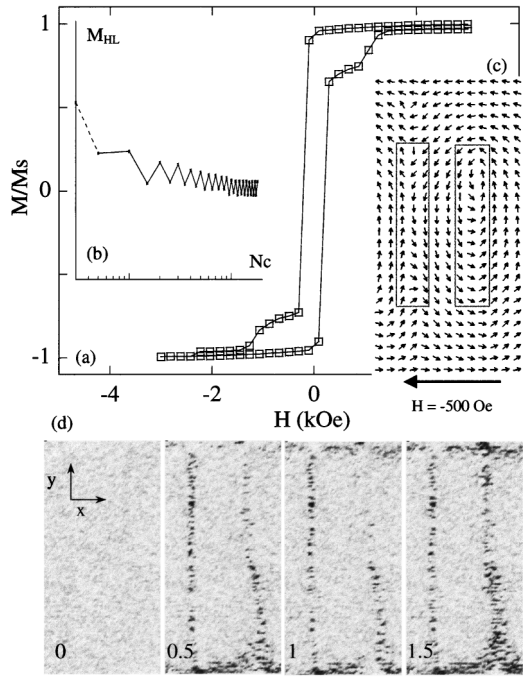

FIG. 4. Micromagnetic simulations of the hard/soft CoPtCr/Cr/Co sandwich. (a) Hysteresis loop of the entire structure. (b) Hard layer remanent magnetization M_{HL} upon cycling the soft layer's magnetization in ± 500 Oe. The variation shown is about 20% of the initial magnetization. (c) Domain structure of the soft layer during the magnetization reversal for an applied field $H = -500$ Oe. Note that the domain wall is propagating from top to bottom. (d) Zero-field domain structure of the hard layer after the first few cycles of the soft layer. White regions (black) indicate magnetic domains pointing along x $(-x)$. The light gray pattern is a consequence of the randomness of the anisotropy directions of the CoPtCr grains.

reversal of the Co layer towards its initial orientation has little effect on this domain structure (1 cycle). The next cycle induces a broadening of the reversed domains parallel to the magnetization (1.5 cycles) due to dipolar interactions. Note that the high contrast which appears along the top and bottom edges of the sample is an artifact of the pinning of the Co magnetization used to generate the DW. The magnetization profile within the Co soft layer during the magnetization reversal [Fig. 4(c)] exhibits a complex DW structure similar to a cross-tie wall [16]. The (horizontal) DW contains both vortexlike and crosslike singularities, indicated by the right and left boxes, respectively, in Fig. 4(c). During the Co layer's magnetization reversal, these two singularities propagate from top to bottom (and vice versa) and induce the formation of the vertical strands of reversed moment in the hard layer as shown in Fig. 4(d). Moreover, closer inspection of the micromagnetics of such a cross-tie DW reveals that in-plane stray fields parallel to the applied field are generated in opposite directions along the top and bottom edges of the singularities within the DW. During the reversal, the magnetization profile of these singularities becomes asymmetric, favoring stray fields in only one direction. This is illustrated in Fig. 4(c) for the case of a negative applied field (i.e., DW propagating from top to bottom): the net magnetization of the vortex (right box) is nonzero along the x direction, generating stray fields pointing to the left (negative). On the contrary, when a positive field is applied, inducing the motion of the DW from bottom to top, the net magnetization of the vortex will be reversed, and so will the stray fields. Thus the domain wall stray fields will point in opposite directions depending on whether the magnetization is switched back or forth, being either "demagnetizing" or "magnetizing" and inducing the oscillatory decay observed experimentally.

In summary, we have observed an oscillatory magnetization decay in a hard CoPtCr layer upon cycling of a neighboring soft magnetic layer. PEEM experiments allow the observation of the domain structure of the hard layer during the demagnetization process. The images exhibit the same oscillatory decay on a microscopic scale. Micromagnetic simulations suggest that this behavior is related to the motion of vortices within the soft layer during its magnetization reversal.

This research was partially supported by DARPA-ONR and MURI. The PEEM work was supported by the Director, Office of Basic Energy Sciences, U.S. Department of Energy under Contract No. DE-AC03-76SF00098. The micromagnetic simulations were made using a program supplied by LLG Micromagnetics Simulator™ and we thank Mike Scheinfein for help with this code.

[1] S. S. P. Parkin, Phys. Rev. Lett. **71**, 1641 (1993).
[2] P. Bruno, Phys. Rev. B **52**, 411 (1995).
[3] S. S. P. Parkin *et al.*, J. Appl. Phys. **85**, 5828 (1999).
[4] Y. Lu *et al.*, Appl. Phys. Lett. **70**, 2610 (1997); K. S. Moon, R. E. Fontana, and S. S. P. Parkin, Appl. Phys. Lett. **74**, 3690 (1999).
[5] L. Néel, C. R. Acad. Sci. **255**, 1676 (1962); S. Demokritov *et al.*, Phys. Rev. B **49**, 720 (1994).
[6] S. Gider, B.-U. Runge, A. C. Marley, and S. S. P. Parkin, Science **281**, 797 (1998).
[7] L. Thomas, M. G. Samant, and S. S. P. Parkin, Phys. Rev. Lett. **84**, 1816 (2000).
[8] Note that in structures containing exchange-coupled FM/antiferromagnetic(AFM) bilayers large internal exchange fields are generated at the FM/AFM interface which can be manipulated by changing the moment of the FM layer in small magnetic fields—see P. A. A. van der Heijden *et al.*, Appl. Phys. Lett. **72**, 492 (1998).
[9] M. R. McCartney *et al.*, Science **286**, 1337 (1999).
[10] J. Stöhr *et al.*, Science **259**, 658 (1993).
[11] S. S. P. Parkin, Mater. Res. Soc. Symp. Proc. **231**, 145 (1992).
[12] J. Stöhr *et al.*, Surf. Rev. Lett. **5**, 1297 (1998).
[13] S. Anders *et al.*, Rev. Sci. Instrum. **70**, 3973 (1999).
[14] Q. Peng *et al.*, IEEE Trans. Magn. **31**, 2821 (1995).
[15] M. R. Scheinfein *et al.*, Phys. Rev. B **43**, 3395 (1991).
[16] D. J. Craik and R. S. Trebble, in *Ferromagnetism and Ferromagnetic Domains* (John Wiley and Sons, New York, 1965), p. 215.